Long Title: Myxoma virus lacking the host range determinant M062 stimulates cGAS-dependent type 1 interferon response and unique transcriptomic changes in human macrophages

Short Title: Myxoma virus subdues type 1 interferon responses through a host range determinant

Authors

Steven J Conrad[1], Erich A Peterson[2], Jason Liem[2], Richard Connor[1], Bernice Nounamo[1], Martin Cannon[1], Jia Liu[1,3]*

*Corresponding author

Email: jliu4@uams.edu

Affiliations

[1]Department of Microbiology and Immunology, University of Arkansas for Medical Sciences (UAMS), Little Rock, AR, USA

[2]Winthrop P. Rockefeller Cancer Institute, University of Arkansas for Medical Sciences, Little Rock, AR, USA

[3]Center of Pathogenesis and Host Inflammatory Responses, University of Arkansas for Medical Sciences (UAMS), Little Rock, AR, USA

Authorship

SC, EAP, JL, RC, BN, and JL* (* responsible author) performed the experiments, MC and JL* provided material, JL* provided funding support for the study, and JL* conceived and designed experiments. JL* wrote and collected comments from other authors to finalize manuscript.

Abstract

The evolutionarily successful poxviruses possess effective and diverse strategies to circumvent or overcome host defense mechanisms. Poxviruses encode many immunoregulatory proteins to evade host immunity to establish a productive infection and have unique means of inhibiting DNA sensing-dependent type 1 interferon (IFN-I) responses, a necessity given their dsDNA genome and exclusively cytoplasmic life cycle. We found that the key DNA sensing inhibition by poxvirus infection was dominant during the early stage of poxvirus infection before DNA replication. In an effort to identify the poxvirus gene products which subdue the antiviral proinflammatory responses (e.g., IFN-I response), we investigated the function of one early gene that is the known host range determinant from the highly conserved poxvirus host range *C7L* superfamily, myxoma virus (MYXV) M062. Host range factors are unique features of poxviruses that determine the species and cell type tropism. Almost all sequenced mammalian poxviruses retain at least one homologue of the poxvirus host range *C7L* superfamily. In MYXV, a rabbit-specific poxvirus, the dominant and broad-spectrum host range determinant of the *C7L* superfamily is the *M062R* gene. The *M062R* gene product is essential for MYXV infection in almost all cells tested from different mammalian species and specifically inhibits the function of host Sterile α Motif Domain-containing 9 (SAMD9), as *M062R*-null (Δ*M062R*) MYXV causes abortive infection in a SAMD9-dependent manner. In this study we investigated the immunostimulatory property of the Δ*M062R*. We found that the replication-defective Δ*M062R* activated host DNA sensing pathway during infection in a cGAS-dependent fashion and that knocking down SAMD9 expression attenuated proinflammatory responses. Moreover, transcriptomic analyses showed a unique feature of the host gene expression landscape that is different from the dsDNA-stimulated inflammatory state. This study establishes a link between the anti-neoplastic function of SAMD9 and the regulation of innate immune responses.

Author Summary

Poxviruses encode a group of genes called host range determinants to maintain or expand their host tropism. The mechanism by which many viral host range factors function remains elusive. Some host range factors possess immunoregulatory functions responsible for evading or subduing host immune defense mechanisms. Most known immunoregulatory proteins encoded by poxviruses are dispensable for viral replication *in vitro*. The uniqueness of MYXV *M062R* is that it is essential for viral infection in vitro and belongs to one of the most conserved poxvirus host range families, the *C7L* superfamily. There is one known host target of the MYXV M062 protein, SAMD9. SAMD9 is constitutively expressed in mammalian cells and exclusively present in the cytoplasm and has an anti-neoplastic function. Humans with deleterious mutations in SAMD9 present disease that ranges from lethality at a young age to a predisposition to myelodysplastic syndromes (MDS) that often require bone marrow transplantation. More importantly, SAMD9 serves as an important antiviral intrinsic molecule to many viruses. The cellular function of SAMD9 remains unclear mostly due to the difficulty of studying this protein, i.e., its large size, long half-life, and its constitutive expression in most cells. In this study we used M062R-null MYXV as a tool to study SAMD9 function and report a functional link between SAMD9 and the regulation of the proinflammatory responses triggered by cGAS-dependent DNA sensing.

Introduction

Mammalian hosts have sophisticated regulation for the triggering of pro-inflammatory responses, especially after detecting danger signals in the cytoplasm. Many fundamental sensing instruments and their direct downstream signaling axes have been described, such as cGAS/STING/IRF3 axis for DNA sensing (1-3) and RNA sensing pathways (4) e.g., the RIG-I/MAVS/IRF3 axis (5). Additional factors may fine-tune the consequences of dangerous stimulus (e.g., DNA substrates) resulting in distinctive overall cellular and immunological responses. The outcome may also be tissue- and cell-type dependent. We are particularly interested in

74 understanding the immunoregulatory mechanism of monocytes/macrophages. These immune
75 cells are among the first responders to viral infection and also important in the maintenance of
76 immunological microenvironment, such as the tumor environment.

77 Cytoplasmic surveillance for the presence of DNA is an important task for mammalian cells, as
78 the appearance of DNA in this privileged compartment signals grave danger for the well-being
79 of the cell. Poxviruses inhibit DNA sensing at an early time during infection and poxviruses from
80 different genera have evolved unique strategies to circumvent host surveillance against
81 cytoplasmic DNA. Here we investigated the phenomenon associated with transcriptomic
82 landscape remodeling in macrophages triggered by a mutant MYXV, Δ*M062R*, and found it
83 distinct from the classic DNA sensing which triggers the type 1 interferon (IFN-I) response.
84 Interestingly, Δ*M062R* induced proinflammatory effect is also regulated by another host protein,
85 SAMD9. This unusual inflammatory response induced by Δ*M062R* may explain the
86 immunotherapeutic benefit we have observed when using Δ*M062R* in the tumor environment (6)
87 and when treating tumor associated macrophages (TAMs) from human patients (unpublished
88 data).

89 Poxviruses are exemplary probing tools in our quest to understand the host immune
90 response(s) at the molecular and pathogenesis levels. Poxvirus must be able to evade host
91 surveillance against cytoplasmic DNA due to their exclusive cytoplasmic life cycle to replicate
92 their dsDNA genome. It is not surprising that many genes encoded by poxviruses antagonize
93 DNA sensing-stimulated antiviral immune responses. In this study we utilized MYXV, a rabbit-
94 specific poxvirus, to investigate novel host regulation of innate immune responses using a viral
95 protein, M062, as a probing tool. Viral M062 protein is essential for MYXV infection with a
96 classic role as host range determinant. M062 has a known host target, SAMD9, and inhibition of
97 SAMD9 is required for a productive viral infection (7, 8). We observed that infection by the
98 replication-defective Δ*M062R* in monocytes/macrophages led to IFN-I induction and the

production of pro-inflammatory cytokines/chemokines. This proinflammatory response associated host gene expression is IRF-dependent and is regulated through DNA sensing by cGAS. The pro-inflammatory responses caused by Δ*M062R* are also regulated by SAMD9, the direct target of viral M062 protein. Interestingly, this dual regulation leads to a unique transcriptomic landscape distinct from that is induced by DNA sensing alone. We thus concluded that this additional regulation of the cGAS DNA sensing pathway through SAMD9 may act to fine-tune the consequences of DNA sensing. This finding elucidates the immunoregulatory function of SAMD9 in addition to its anti-neoplastic property and may explain the role of SAMD9 in host defense against dangerous signals.

Results

Early poxvirus proteins play dominant roles in suppressing dsDNA-stimulated IFN-I

Poxviruses, especially virulent poxviruses, must inhibit the host DNA sensing pathway and IFN-I production to be able to effectively replicate and spread to other cells (9). Many orthopoxviruses encode a poxvirus immune nuclease (poxin), an early poxvirus gene, for cGAS-STING-specific immune evasion (10-13), but poxviruses from non-orthopoxvirus genera may not possess such genes in their genomes, and one example is MYXV. It was reported previously that the gene product of *F17R*, a late gene, from vaccinia virus (VACV) was important for inhibiting DNA sensing (14, 15) and a homolog of the VACV *F17R* is present in MYXV, *M026R* (16). Our early experiment aimed to rule out the possibility that any early viral genes from MYXV might play a role in the inhibition of DNA sensing with VACV WR as a control. Using a well-established IRF-dependent luciferase system in macrophages in the presence of a DNA replication inhibitor, cytosine arabinoside (AraC), we found MYXV infection at the early state could already potently inhibit dsDNA-stimulated luciferase expression comparably to the ability by VACV (**Figure 1A**). The levels of inhibition in the presence of AraC from both VACV and MYXV are similar to those caused by corresponding viruses without AraC treatment (**Figure 1A**). Thus, additional viral

124 factors that are expressed during early gene expression play dominant roles in the suppression
125 of DNA-induced IFN-I induction in MYXV. Next, we found that infection by a replication defective
126 virus with the essential host range gene *M062R* deleted, Δ*M062R*, lost the ability to inhibit
127 dsDNA-stimulated IFN-I induction (**Figure 1B**). It is known that Δ*M062R* infection retains other
128 early viral gene expression comparable to what is seen in the wildtype MYXV infection (7).

129 <u>*M062R*-null MYXV (Δ*M062R*) infection stimulates proinflammatory cytokine production</u>

130 The MYXV early gene, *M062R*, is a broad-spectrum host range determinant from the poxvirus
131 host range *C7L* superfamily (17) and is essential for MYXV infection (7, 8). The Δ*M062R* MYXV
132 has a tropism defect and causes an abortive infection in almost all cells tested from species
133 such as humans and rabbits (7). Both viral DNA replication and late protein synthesis are
134 significantly inhibited causing abortive infection during Δ*M062R* infection, while early gene
135 expression remain intact (7). The virotherapeutic benefit we observed prompted us to
136 investigate the immunological effect caused by Δ*M062R* (18), since this mutant virus is unable
137 to establish a productive viral replication and oncolytic effect of Δ*M062R* is not through direct
138 induction of cell death, e.g., apoptosis. We performed a RT^2 profiler screening for antiviral
139 responses to compare how responses generated by Δ*M062R* infection differed from the
140 wildtype MYXV infection. We found Δ*M062R* infection in human primary monocytes stimulated
141 the expression of many antiviral and interferon-stimulated genes (ISGs) (**Figure 2A**). To
142 validate the above findings from the screening we collected periphery blood from 4 healthy
143 individuals and purified $CD14^+$ monocytes/macrophages for RT^2-PCR confirmation. We found
144 Δ*M062R* infection in these cells generally stimulated elevated IFN-I and ISGs, e.g., IFN β and
145 CXCL-10 (**Figure 2B**), consistent with the screening results. We also confirmed the elevated
146 CXCL-10 levels in the supernatant of Δ*M062R* infected cells (**Figure 2C**). As a control we
147 included a MYXV deletion mutant in which another *C7L* superfamily gene, *M063R*, was ablated,
148 *M063R*-null MYXV (19). *M063R*-null MYXV remains replication-competent in human cells and

M063R does not possess a broad-spectrum host range function (17, 19). In our study, the control *M063R*-null MYXV infection did not induce IRF-dependent luciferase expression (not shown), and similar to the wildtype virus *M063R*-null MYXV did not cause upregulation of CXCL10 in human $CD14^{+}$ macrophages (**Figure 2C**).

The Δ*M062R* stimulated IRF-dependent gene expression is sensed through cGAS

We have reported previously that the infection defect by Δ*M062R* was due to its inability to overcome host SAMD9 function (8). However, the immunological impact of Δ*M062R* remains unknown. A computational analysis of SAMD9 across all homologues found putative DNA binding domains (20), and DNA pulldown experiments using either the VACV 70mer dsDNA (21) or herring testes dsDNA (not shown) indicated that SAMD9 was co-immunoprecipitated with dsDNA (**Figure 3A**). We found previously that the MYXV M062 protein binds to amino acids (aa) 1-385 of human SAMD9 but not to the first 285 aa residues or c-terminal portion of SAMD9 (18), while the region of 285-385 aa in human SAMD9 overlaps with the putative DNA binding domain, the Alba-2 domain (20). We next examined if a human SAMD9 1-385 aa fragment could also be associated with dsDNA. We used the *SAMD9*-null HeLa cells we previously engineered (18) for the experiment and by transiently transfecting the cells to express SAMD9 1-385 aa we performed dsDNA pulldown experiment similar to what is shown in Figure 3A. We found that the SAMD9 1-385 aa truncated protein also associated with dsDNA. As a control, we transiently expressed a SAMD9 N-terminal fragment of 1-110 aa that contains the SAM domain in *SAMD9*-null cells, and found that this SAMD9 fragment was not associated with DNA. We then investigated whether the expression of MYXV M062 might interfere with SAMD9's presence in the dsDNA pulldown content. As a control, we infected HeLa cells expressing intact endogenous SAMD9 with either wildtype MYXV or Δ*M062R*. Wildtype MYXV infection significantly reduced the amount of SAMD9 associated with dsDNA compared with that from Δ*M062R* infection (**Figure 3C**).

Considering that SAMD9 may function through forming a complex with factors binding to DNA, we decided to test whether the ability of Δ*M062R* to induce IFN-I is due to the activation of DNA sensors. We utilized a luciferase expression in human monocytic THP-1 cells for the study. THP-1 cells can be differentiated into macrophages for testing DNA sensing and downstream outcome, and the firefly luciferase (F-Luc) expression is driven by the IRF recognition domain (Invivogen, San Diego, CA) (22). To test whether DNA sensing plays a role in Δ*M062R*-induced IFN-I induction and pro-inflammatory responses, we used cGAS-null THP-1 cells that were engineered from the F-Luc expressing parental cells mentioned above (22). We found that Δ*M062R* mutant virus stimulated robust luciferase expression comparable to that induced by interferon-stimulating DNA (ISD) (21) transfection (**Figure 4A**). In the absence of cGAS, the luciferase expression caused by both Δ*M062R* and ISD was eliminated (**Figure 4A**). However, transfection of 2'3'-cGAMP, the messenger molecule generated by cGAS upon DNA binding, successfully bypassed the lack of cGAS in cGAS-null THP-1 to restore F-Luc expression (**Figure 4B**). We thus conclude that the immunostimulatory effect of Δ*M062R* is due to the activation of cGAS-dependent DNA sensing pathway.

Knocking down SAMD9 expression in monocytes/macrophages attenuated their proinflammatory responses

MYXV M062 inhibits SAMD9 function, leading to a productive viral infection. We next examined whether SAMD9 played a role in regulating the proinflammatory responses induced by Δ*M062R*. We generated stable SAMD9 knock-down THP1 cells using lentivirus expressing shRNAs targeting human SAMD9. As control, we engineered THP1 cells stably expressing scrambled shRNAs. We infected differentiated THP1 control or SAMD9 knockdown cells with Δ*M062R* for 18 hrs before examining pro-inflammatory cytokine production via RT-PCR. We found that reduced SAMD9 expression indeed attenuated Δ*M062R*-induced pro-inflammatory responses (**Figure 5A**). Transfection of ISD in these cells showed a similar attenuation in the

IFNβ mRNA levels (**Figure 5B**). However, transfection of 2'3'-cGAMP led to upregulation of the IFNβ and ISG expression in SAMD9-knockdown THP1 cells (**Figure 5C**) that is similar to the response in the control THP1 cells. We thus concluded that Δ*M062R* infection stimulated a unique pro-inflammatory state that is cGAS-dependent and also regulated by SAMD9.

Next generation sequencing showed a unique gene expression profile during Δ*M062R* infection

We conducted a next generation sequencing study in the macrophage-like THP-1 cells to investigate the global transcriptomic change caused by Δ*M062R*. We hypothesized that since Δ*M062R* infection of macrophages stimulated cGAS-dependent IFN-I response, the infection will lead to similar results as dsDNA stimulated changes at the transcriptomic landscape. As control, we included the cells transfected with ISD dsDNA. Using the dual RNAseq bioinformatic analyses, we found that Δ*M062R* infection in monocytes/macrophages stimulated a very different gene expression profile from that of the ISD group (PCA plot **Figure 6A**, Venn diagram **Figure 6B,** and heatmap **Figure 6C**). Ingenuity Pathway Analysis (IPA) confirmed the activation of cGAS pathways by Δ*M062R* infection (IPA graphic summary **Figure 6E**), but additional gene expression profiling suggests a unique alteration of the transcriptomic landscape unlike that of the ISD transfection-induced antiviral response (**Figure 6F**). At the transcriptomic level, Δ*M062R* treatment also showed distinct changes compared to wildtype MYXV infection (**Figure 6D**). Although wildtype viral infection inhibited IRF3-dependent gene expression, it stimulated an unusual subgroup of chemokine/cytokine production in the macrophages (IPA graphic summary **supplemental Figure 1**).

We next compared the viral gene expression pattern at 8 hours post-infection between Δ*M062R* mutant virus and wildtype MYXV. Surprisingly, in the Δ*M062R* infection we detected all the viral genes expressed in the wildtype MYXV infection (**Supplemental Figure 2**). We found 57 viral genes in Δ*M062R* infection were differentially expressed compared to wildtype MYXV with statistical significance (p value ranging from 1.03e-03 to 2.72e-88). Most of them (52 viral

genes) (**Table 2**) showed slightly higher levels in Δ*M062R* infection than that in wildtype MYXV infection. *M136R* expression in the Δ*M062R* infection is 2.6-fold (logFC=1.4) higher than that expressed in wildtype MYXV infection (**Table 2**). Only 5 viral genes showed significant reduction at RNA levels during Δ*M062R* infection compared to that in wildtype MYXV infection. Among these viral genes, only *M062R* transcript was noticeably reduced (logFC=-3.95) due to the deletion of the central 80% of the *M062R* coding sequence (7) (**Supplemental Figure 3**) and the reduction in the levels of the remaining viral genes are in the range of 0.44-0.64 (logFC between -1.16 and -0.652) (**Table 2**).

Discussion

Poxviruses are large dsDNA viruses with an exclusively cytoplasmic life cycle. These viruses can effectively inhibit IFN-I induction through many strategies. These strategies include blocking IFN-I signaling through decoy receptors (23), inhibiting key signaling effector molecules of the sensing pathways (9, 11), and/or reprograming host gene expression in the nucleus (24-26). One critical ability is for mammalian poxviruses, especially virulent poxviruses, to circumvent host immunosurveillance and the antiviral immune responses induced as a result of DNA sensing (9). Myxoma virus belongs to the genus of *Leporipoxvirus* and has a narrow host tropism, causing infectious disease only in rabbits. In European rabbits, virulent MYXV can cause lethal infection with 100% lethality and profound immunosuppression (27). Despite its limited host tropism for infectious disease, we found wildtype MYXV inhibits the DNA sensing pathway in human cells comparably to VACV, suggesting the presence of an antagonistic mechanism directed against host DNA sensing in a species-independent manner.

Host detection of cytoplasmic DNA by the cyclic GMP-AMP synthase (cGAS) leads to the production of the second messenger molecule 2’3’-cGAMP; binding of cGAMP to the adaptor, a stimulator of interferon genes (STING), triggers the activation of IFN-I production through a series of signaling events involving STING activation, recruitment and activation of TBK1, and

249 phosphorylation of IRF3 (28). Many poxvirus proteins inhibit DNA sensing through different
250 strategies, such as direct degradation of 2', 3'-cGAMP by Poxvins (12, 13), inactivation of
251 STING through mTOR by VACV F17 (15), inhibition of IRF3 by VACV C6 (29), and inhibition
252 NF-κB activation by many VACV proteins including B14 (30) and F14 (31), etc. More
253 importantly, inhibition of host DNA sensing by poxviruses during early infection seems to be a
254 common strategy in spite of their species tropism. Poxvirus early and post-replicative gene
255 expression can be distinguished through the use of a DNA replication inhibitor such as AraC. It
256 is not surprising that poxviruses from different genera diverge on strategies to evade DNA
257 sensing with distinct mechanisms but achieve the same outcome. In the MYXV genome,
258 homologs of Poxvin are not found and a homolog of VACV F17 is predicted to be a late protein.
259 MYXV may encode one or multiple additional early genes uniquely functioning as inhibitors of
260 the DNA sensing pathway. In this study, we identified one MYXV viral protein which functions in
261 such a capacity.

262 The MYXV *M062R* gene belongs to one of most conserved poxvirus host range factor families,
263 the poxvirus *C7L* superfamily (17), and is a host tropism determinant of MYXV essential for viral
264 replication (7). Although MYXV *M062R* can compensate for the function of the VACV *C7L* gene
265 (32), it is predicted to have functional divergency from C7 and other *C7L* family members of
266 orthopoxviruses (17). The MYXV M062 is unique from C7 in that [a] in VACV the *C7L* gene is
267 non-essential and [b] only when *C7L* and another orthopoxvirus host range gene *K1L* are both
268 deleted does the defect in host range tropism (comparable to Δ*M062R* MYXV) and replication
269 deficiency become apparent (33). A known function of the MYXV M062 protein is to inhibit the
270 function of the host protein SAMD9 (7, 8), but direct immunological impact of the MYXV M062
271 protein is not known. More importantly, the immunotherapeutic potential of *M062R*-null MYXV
272 as an adjuvant for cancer therapy (6) further motivated our investigation of its
273 immunostimulatory mechanism. Targeted deletion of *M062R* gene in the MYXV genome

resulted in a mutant virus that maintained early gene expression at the protein levels but showed reduced DNA replication without late viral proteins being detected through western blot (7). Interestingly, in our RNAseq analyses we not only detected post-replicative viral RNA, especially late viral RNAs during Δ*M062R* infection, but also found Δ*M062R* viral RNA synthesis patterns in macrophages closely resembling that of the wildtype MYXV infection. We observed an occasional reduction in RNA levels among a few late genes during Δ*M062R* infection, and most of the Δ*M062R* viral transcripts were present at slightly higher levels than that in the wildtype MYXV infection at the same time point. The presence of significant levels of late RNA during Δ*M062R* infection is unexpected, as in order to synthesize late viral RNA comparable to the wild type virus level, many intermediate proteins must be produced *de novo*. This phenotype suggests a unique antiviral state stimulated by Δ*M062R* MYXV infection. In this state, viral protein synthesis, especially late protein production, is inhibited, which effect is coupled with inhibition of viral DNA replication. We speculate that the unique antiviral effect of inhibiting viral protein synthesis may be connected to the DNA sensing event. An alternative possibility is that the absence of M062 during Δ*M062R* infection may lead to translation deceleration of viral proteins until a complete stop, when a large quantity of late viral proteins are needed to complete the life cycle. In this alternative scenario, the DNA-trigger immune response reported may be caused by suboptimal levels of viral immunoregulatory proteins. This is, however, less probable because of the observed robust IRF-dependent gene expression triggered by Δ*M062R,* comparable to what is directly induced by dsDNA as shown in the luciferase assay.

Cytoplasmic sensing of DNA to trigger protective inflammation plays a key role in host antiviral defense (34, 35). The causes of cytoplasmic DNA may vary during the lifetime of a mammalian cell, such as improperly processed cellular DNA due to DNA repair or replication defect (36), and foreign DNA such as during viral infection (9, 37). Once triggered, DNA sensing induced IFN-I production and inflammation will lead to dramatic changes in the immunological milieu that

299 may ultimately alter the immune responses profoundly. Thus, there must be additional control
300 mechanisms to monitor and then regulate DNA-dependent IFN-I induction. There are known
301 downstream host control mechanisms to fine tune IFN-I responses. Other than negative
302 feedback cascade to restrict the duration and extent of IFN-I responses, e.g., SOCS, regulation
303 of IFN-α receptor (IFNAR), and USP18 (38-40), intracellular signaling events and miRNAs can
304 also perform such function (41). Upstream of IFN-I production, there are also regulatory
305 measures to pattern recognition receptors (PRRs) and their adaptors, e.g., AKT to cGAS (42),
306 TMEM120A to STING (43), and RNF138 to TBK1 (44). Our work provides evidence of a novel
307 mechanism to fine tune the IFN-I response, which may operate through cellular translation
308 regulation to PRR activation (**Figure 7**), and ultimately alters the global transcriptional
309 landscape.

310 SAMD9 is a large and exclusively cytoplasmic protein with complex domain structure,
311 interestingly including putative DNA-binding domains (20). Our study indicated that SAMD9
312 itself is not necessarily a direct DNA sensor, since the triggering of IFN-I induction and
313 subsequent proinflammatory responses is through cGAS-dependent DNA sensing events.
314 During wildtype MYXV infection, cGAS may not have access to MYXV genome DNA in the
315 cytoplasm in order to induce IFN-I. In the presence of M062 protein, SAMD9 is located
316 exclusively outside of the cytoplasmic viral factories (8). However, during Δ*M062R* infection,
317 SAMD9 can be detected abundantly surrounding the viral factories (8). Because of its putative
318 DNA binding domain and its complex domain structure (20), SAMD9 may serve as an enabler to
319 facilitate the access to DNA by sensors such as cGAS. SAMD9 participated in the regulation of
320 host translation in the initiation and plays an important role in the elongation steps (unpublished
321 data), and deleterious mutations in SAMD9 can inhibit global protein synthesis (45). More
322 importantly, SAMD9 may serve as a signaling hub to fine tune the immunological consequences
323 of the cell. SAMD9 may be targeted by other viruses (46) and has broad-spectrum antiviral

effect (47-49). In our pursuit of understanding the mechanism of the SAMD9 antiviral effect, we revealed a key role of SAMD9 in regulating innate sensing for transcriptional remodeling in monocytes/macrophages. This work leads us to investigate its function in connecting innate immune sensing, translation control, and transcriptional refinement in host immune responses in the next step.

Materials and Methods

Cell culture and virus stock

Mammalian cells used in this study include BSC-40 (ATCC CRL-2761) (in Dulbecco minimal essential medium, DMEM, Lonza), healthy human periphery $CD14^+$ monocytes (Lonza, Walkersville, MD), THP1 (ATCC TIB-202), and THP1-Lucia (kindly provided by F. Zhu) (50) (in RPMI1640, Lonza). The complete growth medium (e.g., DMEM Lonza/BioWhittaker Catalog no 12-604Q, or RMPI1640) was supplemented with 10% FBS (Atlanta Biologicals, Minneapolis, MN), 2 mM glutamine (Corning Cellgro, Millipore Sigma, St. Louis, MO), and 100 μg per ml of Pen/Strep (Corning Cellgro, Millipore Sigma, St. Louis, MO); for RPMI1640 complete culture medium, in addition to FBS, glutamine, and Pen/Strep, 2-mercaptoethanol (MP biomedicals, Solon, OH) was supplemented to a final concentration of 0.05 μM.

The viruses used were all derived from myxoma virus (MYXV), Lausanne strain (GenBank Accession AF170726.2). The MYXV *M062R* deletion mutant (vMyxM062RKOgfp) has been described previously (7). Myxoma virus stocks were prepared on BSC-40 cells and purified with sucrose step gradient through ultracentrifugation as previously described (51).

RT^2 Profiler PCR Array and Multi-plex Cytokine Array

Primary human $CD14^+$ monocytes/macrophages (Lonza, Walkersville, MD) were mock treated, infected with wildtype MYXV and vMyxM062RKOgfp at a multiplicity of infection (moi) of 5 for 16 hours (hrs) before harvesting RNA for RT Realtime (RT^2) PCR profiler and collecting

supernatant for the Multi-plex Array study. For RT^2 Profiler PCR Array Human Interferons and Receptors (Cat# PAHS064ZC-12, Qiagen, Germantown, MD), RNA extraction (RNeasy Pls Mini kit, Qiagen), cDNA synthesis (RT^2 First Strand Kit, Qiagen), and Realtime PCR (RT^2 SYBR Green qPCR Mastermixes, Qiagen) were performed following standard instructions from the manufacturer. The result is representative data from 1 individual and a total of 2 healthy individuals' $CD14^+$ monocytes which were tested (biological replicates). For Cytokine Multiplex of Human Inflammation Panel (Invitrogen™ Inflammation 20-Plex Human ProcartaPlex™ Panel) (Catalog # EXP20012185901, eBioscience/Invitrogen) procedures were performed following manufacturer protocol and the plate was processed on BioRad Bio-Plex 200 system with Bio-Plex-HTF attachment (Bio-Rad, Hercules, CA). The result is the representative from one individual's $CD14^+$ samples and a total of 2 healthy individuals' $CD14^+$ monocytes were tested. Shown is the average intensity from duplicate samples (technical replicates).

Purification of human periphery $CD14^+$ monocyte/macrophage

Healthy human whole blood was collected by venous puncture into collection tubes (BD catalog# 364606, Vacutainer ACD Solution), approximately 8 mL of whole blood per tube. An equal volume of sterile, room-temperature Dulbecco's Phosphate Buffered Saline without calcium and magnesium (DPBS) (Corning catalog# 21-031-CV) was added to the flask. The diluted whole blood was layered over Lymphoprep solution (Accurate Chemical and Scientific Corp., Catalog# 1114545) and centrifuged at 2,500 rpm for 20 minutes. The collected PBMCs were 1:1 diluted with DPBS. The tube was then centrifuged at 1500 rpm for 5 minutes and the cell pellet was resuspended in 20 mL DPBS before repeating the wash process once more. The pellet was resuspended in 0.5 mL DPBS with 0.5 % BSA and labeled with 50 µL anti-CD14 microbeads (Miltenyi Biotec, catalog# 130-050-201). Cells were labeled for at least 20 minutes at 4 °C and $CD14^+$ cells were isolated by magnetic column (Miltenyi Biotec, catalog# 130-042-201).

373 Luciferase assay

374 Supernatant from each sample was collected and immediately used in the luciferase assay.
375 Luciferase presence in the supernatant was quantified by kit (QUANTI-luc, InvivoGen, catalog
376 number rep-qlc1). Each sample was tested in triplicate in white 96-well plates with clear bottoms
377 (LUMITRAC 200, Greiner Bio-One, Monroe, NC) with 5 times of volume to the supernatant
378 sample. For each sample in triplicate the arithmetic average was reported. Fold induction is
379 calculated as previously reported (9).

380 Semi-quantitative RT Realtime PCR

381 THP-1 cells (10^6 cells per 3.5 cm dish) were differentiated in PMA at 50 ng/mL for 48 hours (hrs)
382 before being mock treated, transfected with ISD (21) at 2 μg per dish using ViaFect (Promega,
383 Madison, WI) at 3 μL per 1 μg of ISD based on manufacturer protocol, or infected at an moi of 5
384 for either WT (vMyxGFP) or *M062R*-null MYXV (7). At 1 hour (h) and 8 hrs post-transfection for
385 ISD or 1 hr and 12 hrs post-infection, cells were harvested with Direct-zol RNA Mini Prep kit
386 (catalog # R2052, Zymo, Irvine, CA) according to manufacturer standard protocol. RNA quality
387 is examined by running on the RNA gel to check 28S and 18S integrity and spectrophotometer
388 to estimate concentration. Equal amount of total RNA in a maximal volume of 6 μL is used for
389 cDNA synthesis using NEB PhotoScript® First Strand cDNA Synthesis Kit (Catalog # E6300L,
390 NEB Inc, Ipswitch, MA) as instructed in the manufacturer standard protocol. Realtime PCR is
391 conducted following manufacturer standard protocol (Luna Universal qPCR Master Mix, NEB
392 Inc). Sybr green RT-PCR primers used in this study is listed in Table 1.

393 Generation of SAMD9 knockdown and control THP1 cells

394 Lentiviral particles for stable SAMD9 shRNA expression (Cat# sc-89746-V, Santa Cruz
395 Biotechnology, Dallas, TX) and Lentiviral particles for stable expression of scramble shRNAs
396 (Santa Cruz Biotechnology, Dallas, TX) were used for generating the cell lines. We followed the

manufacturer's standard protocol similar to that reported before (7), and stable expression was selected under puromycin at 5 μg/mL. SAMD9 knock-down was confirmed by Western Blot using rabbit anti-SAMD9 antibody (Cat# HPA021319, Millipore-Sigma, St. Louis, MO) and goat-anti-rabbit HRP secondary antibody (Cat# 111-035-144, Jackson ImmunoResearch Laboratory, INC, West Grove, PA) according to manufacturer's instructions.

Next Generation RNA sequencing

THP-1 cells (10^6 cells per 3.5 cm dish) were differentiated in phorbol myristic acid (PMA) (Millipore-Sigma) at 50 ng/mL for 48 hours before mock treated, transfection with ISD (21) at 2 μg per dish using ViaFect (Promega, Madison, WI) at 3 μL per 1 μg of ISD based on manufacturer recommendations, or infected at an moi of 5 for either WT (vMyxGFP) or *M062R*-null MYXV (7). At 8- hour post-transfection of ISD and at 1- and 8- hour post-viral infection cells were harvested, pelleted by centrifugation and then stored in -80°C until RNA extraction. RNA was extracted using the Quick DNA/RNA Mini-Prep Plus kit (catalog # D7003; Zymo, Irvine, CA, USA) with on-column DNase digestion. Purified RNA was assessed for mass concentration using the Qubit RNA BR Assay kit (catalog # Q10211; Invitrogen, Waltham, MA, USA) and for integrity using the Standard Sensitivity RNA Analysis kit on a Fragment Analyzer capillary electrophoresis system (catalog # DNF-471-0500; Agilent, Santa Clara, CA, USA). A total of 250ng total RNA was used for each sample as input to the TruSeq Stranded Total RNA library prep kit with unique-dual indexing (catalog #s 20020598 & 2002371; Illumina, San Diego, CA, USA). Libraries were assessed for mass using the Qubit 1X dsDNA HS Assay kit (catalog # Q33231; Invitrogen, Waltham, MA, USA), for fragment size using the High Sensitivity NGS Fragment Analysis kit on a Fragment Analyzer capillary electrophoresis system (catalog # DNF-474-0500; Agilent, Santa Clara, CA, USA), and functional validation using the Universal Library Quantification kit (catalog # 07960140001; KAPA, Wilmington, MA, USA).

Validated libraries were adjusted to 3nM before pooling, denaturing, and clustering. Paired-end (2X75) sequencing was performed to an average of 40 million reads per sample on a HiSeq 3000 (Illumina, San Diego, CA, USA).

Dual RNAseq data processing and Ingenuity Pathway Analysis (IPA)

Raw Illumina binary base call (BCL) files were demultiplexed, adapter trimmed, and transformed to paired-end FASTQ files using bcl2fastq v2.18.0.12 (52). FastQC v0.11.4 (53) was then used to assess the quality of the FASTQ files. A "hybrid" *H. sapien* (Ensembl GRCh37 build) and Myxoma virus (Lausanne strain, NCBI, NC_001132.2) reference genome was constructed. FASTQ files for each sample were aligned to the hybrid genome using STAR v2.7.6a (54) and run in its two-pass mode. STAR alignment metrics and QualiMap v2.2.1 (55) were used to assess alignment quality.

StringTie v2.1.4 (56) was then used to perform transcriptome reconstruction using each sample's BAM file. Options were set to only allow the reconstruction and quantification of annotated genes. The gene reference general feature format (GTF/GFF) was produced. Additionally, options were provided to output "Ballgown-ready" files.

For gene-level exploratory data analysis (EDA) and differential expression analysis, StringTie output was imported into DESeQ2 v1.32.0 (57), where p-value and adjusted p-value thresholds were set to 0.05 and 0.1, respectively.

Differential gene expression analysis (e.g., *M062R*-null MYXV infection vs. mock and wildtype MYXV infection vs. mock) was uploaded for IPA to host pathway core analyses, and graphic summary was exported for data presentation.

Statistical analyses

Graphpad Prism 9.1 was used for statistical analyses. Multiple-group comparison with single variable was performed using One-way ANOVA followed by secondary comparisons (e.g., Tuckey multiple comparisons test). Statistical significance is defined by a $p<0.05$.

Acknowledgements

The study was supported by NIH K22AI099184 and R01AI139106 to J.L., a fund from the River Valley Ovarian Cancer Coalition, and a start-up by UAMS Department of Microbiology and Immunology to J.L. M.C. was supported by NIH P50 CA136393-11, Mayo Clinic SPORE in ovarian cancer. This work is also supported in part by the Center for Microbial Pathogenesis and Host Inflammatory Responses grant P20GM103625 through the NIH National Institute of General Medical Sciences (NIGMS) Centers of Biomedical Research Excellence (COBRE) and by the Winthrop P. Rockefeller Cancer Institute at UAMS. We would like to thank Jianmei Chen, Shana Chancellor, Pratikshya Paudel, and especially Sarah Blair for their technical support.

Legends

Figure 1. Myxoma virus *M062R* gene is important for viral inhibition of DNA sensing. A. Early gene expression from either wildtype MYXV or VACV inhibits dsDNA-stimulated IFN-I induction. The IRF-dependent luciferase-expressing THP-1 cell line is a surrogate system for IFN-I induction. After cells were differentiated into macrophages, viral infection was performed at an moi of 10 in the presence of AraC (100 μM) before cells were transfected with HT-DNA. In the absence of post-replicative gene products due to AraC treatment, wildtype MYXV or VACV infection significantly inhibited dsDNA-stimulated luciferase expression. Statistical analyses were performed with ordinary one-way ANOVA followed by Tukey's multiple comparison test and $p<0.05$ is defined as being statically significant (****$p<0.0001$). Shown is a representative result of 2 biological replicates and each data point is an average of triplicate measurements (technical replicates). **B.** In the absence of *M062R* gene, the resulting Δ*M062R* MYXV loses the ability to inhibit HT-DNA stimulated luciferase expression. The same luciferase-expressing THP-1 cells were differentiated into macrophages as in "**A**". After viral infection at a high moi of 10 with VACV or MYXV, cells were transfected with HT-DNA for 18 hrs. Supernatant was then collected to measure the luciferase activities. *M062R*-knockout MYXV could no longer inhibit

dsDNA-stimulated IRF-dependent luciferase expression. Statistical analyses were performed using ordinary one-way ANOVA followed by Dunnett multiple comparison test and $p<0.05$ is defined as being statistically significant (****$p<0.0001$). Shown is a representative of 3 biological replicates and each data point is the average of 2 replicating measurements.

Figure 2. Infection by Δ*M062R* MYXV stimulates the expression of interferon-stimulated genes (ISGs). A. Infection by Δ*M062R* MYXV stimulates higher levels of IFN and ISG RNAs in primary human $CD14^+$ monocytes than that from the wildtype MYXV infection. Infection by MYXV, wildtype and Δ*M062R*, was performed at an moi of 10 and cells were collected at 16 hours post-infection (p.i.) for RNA extraction, reverse transcription, and RT-PCR according to the manufacturer's protocol. The ΔCt and ΔΔCt was calculated and RNA levels were normalized to an internal control gene, B2M. By normalizing to the result of the mock infected group for the same gene, fold induction of the corresponding gene is calculated using the formula of Foldchange=2^(-ΔΔCt). Shown is representative data from one of two healthy donors. **B**. Validation of RT^2-PCR by Δ*M062R* leads to upregulation of IFN-I and pro-inflammatory molecules in CD14. Primary $CD14^+$ human monocytes from 4 healthy human donors were mock infected or infected with either wildtype or Δ*062R* MYXV. In each case the expression of mRNAs encoding several ISGs including CXCL-10, ISG54 and MX-1 were elevated in the monocytes/macrophages infected with Δ*M062R* MYXV compared to monocytes/macrophages infected with wild type MYXV. Fold changes are measured by normalizing to that of mock infection. **C**. Infection by Δ*M062R* can no longer inhibit DNA-sensing pathway. As a control for viral manipulation the *M063R*-null MYXV was used to infect primary $CD14^+$ human monocytes along with other controls (mock infection and wildtype MYXV) and Δ*M062R* infection. CXCL-10 production in the supernatant is shown and the Δ*M062R*-infected monocytes/macrophages secreted significantly higher levels of CXCL-10 than control groups.

Figure 3. Viral M062 prevents human SAMD9 from being associated with dsDNA. A. DNA pull-down assay shows SAMD9 associated with dsDNA. HeLa cell lysate was incubated with either pre-conjugated Streptavidin UltraLink Resin with 5'-biotinylated VACV 70mer dsDNA or un-conjugated Streptavidin Resin alone. After extensive washing, resin-associated content was eluted for Western blot analysis by probing for SAMD9. Lane 1: 5'-biotinylated VACV 70mer dsDNA with resin; Lane 2: resin alone. **B.** SAMD9 1-385 aa domain but not the N-terminal 1-110 aa is associated with dsDNA. The same 5'-biotinylated VACV 70mer dsDNA pull-down experiment as in "A" is performed. Cell lysate from mock transfected, 1-110 aa construct (FLAG tagged) transfected, or 1-385 aa (FLAG tagged) construct transfected cells were used to incubate with dsDNA (VACV 70mer) conjugated resin and the co-precipitated content was separated on SDS-PAGE and probed for FLAG by Western Blot. **C.** The presence of M062 inhibits the association of SAMD9 with dsDNA. With the same dsDNA probe described above, we used HeLa cells expressing endogenous SAMD9 and infected them with either wildtype MYXV expressing V5 tagged M062 protein or Δ*M062R* MYXV for dsDNA pull-down assay. Proteins associated with DNA were separated on SDS-PAGE for Western Blot probing for SAMD9 and V5 tagged M062. The input lysates were examined for total SAMD9 expression.

Figure 4. IRF-dependent gene expression stimulated by Δ*M062R* MYXV is regulated through cGAS.

A. Infection by Δ*M062R* MYXV stimulates similar IRF-dependent gene expression to dsDNA-stimulated effect and is cGAS- dependent. THP-1-Lucia human macrophages with or without cGAS expression were treated by transfection with interferon-stimulated dsDNA (ISDs) or by infection with Δ*M062R* MYXV. Only the THP-1 cells with intact cGAS were able to respond with increased production of luciferase in either treatment. **B.** Addition of 2'3'-cGAMP bypasses the cGAS deficit and induces the production of IFN-I messenger RNA by RT-PCR. Transfection of 2'3'-cGAMP, the enzymatic product from activated cGAS, produces an identical response in

both wild type and cGAS-null THP-1 macrophages, demonstrating that the remainder of the DNA-stimulated IFN-I pathway remains intact.

Figure 5. Knocking down SAMD9 expression attenuates the proinflammatory responses in THP-1 cells induced by Δ*M062R* infection.

A. THP-1 cells in which SAMD9 was knocked down by shRNA. Western blotting showed reduced SAMD9 expression in THP-1 cells stably-transduced with lentivirus expressing SAMD9 shRNAs. **B**. Knocking down SAMD9 expression attenuated the proinflammatory response induced by Δ*M062R*. Compared to control shRNA expressing THP-1, the SAMD9-knockdown cells showed reduced proinflammatory responses after Δ*M062R* infection using RT-PCR. **C**. ISD-stimulated IFNβ mRNA is reduced in SAMD9 knockdown cells. After ISD transfection, IFNβ mRNA is measured by RT^2-PCR and in SAMD9-knockdown cells the expression level of IFNβ is reduced. **D**. Transfection of 2'3'-cGAMP bypasses the block on dsDNA-induced proinflammatory responses in SAMD9-knockdown cells. Transfection of 2'3'-cGAMP in both control and SAMD9-knockdown cells showed similar expression of IFNβ and CXCL-10 mRNA.

Figure 6. Dual RNAseq analyses reveal a unique host transcriptional profile stimulated by Δ*M062R* MYXV infection that is distinct from that caused by dsDNA.

A. PCA plot of mock, ISD, ΔM*062R*, and wildtype MYXV treated samples. Good separation among all four samples are observed with close clustering within replicates. **B.** Venn diagram of host genes identified as being differentially regulated in ISD, ΔM*062R*, and wildtype MYXV groups compared to mock treated cells. Gene lists were generated by performing differential gene expression analysis using the R library DESeQ2, and only those genes whose adjusted-p-value was less than 0.1 were included in the analysis. **C.** Heatmap showing distinct host gene expression profile stimulated by Δ*M062R* from that by dsDNA. All significant differentially expressed genes between 2 groups under study were visualized using the R library heatmap.2. Gene counts were normalized using DESeQ2's default normalization. Each row's values were

scaled using a z-score method before plotting and ward. D hierarchical clustering was performed using the Euclidean distance measure. **D.** Distinct host transcription profiles between ΔM*062R* and wildtype MYXV infection. All significant differentially expressed genes, between the groups under study, were visualized using the R library heatmap.2. Gene counts were normalized using DESeQ2's default normalization. Each row's values were scaled using a z-score method before plotting and ward. D hierarchical clustering was performed using the Euclidean distance measure. **E.** Ingenuity pathway analysis (IPA) revealed signaling pathway stimulated by Δ*M062R* infection. Host genes differentially expressed during Δ*M062R* infection at 8h post-infection were analyzed using IPA (Qiagen, version 01-20-04) for pathways affected. The graphic summary is shown. **F.** ISD transfection leads to activation of classic antiviral responses consistent to dsDNA-stimulated signaling events. Shown is the graphic summary generated by IPA using differentially expressed genes from ISD treatment group at 8-hour time point.

Figure 7. Summary of SAMD9 effect to DNA sensing pathway that is inhibited by viral

Supplemental Figure 1.

IPA analyses revealed unique transcriptional changes in host gene expression stimulated by wildtype MYXV. Host genes differentially expressed in wildtype MYXV infection were analyzed using IPA and a graphic summary of the results is shown.

Supplemental Figure 2.

Venn diagram of MYXV specific genes detected in dual RNAseq analyses. Almost all viral genes expressed by wildtype MYXV at 8 h were detected in ΔM*062R* infection.

Supplemental Figure 3.

Raw data alignment of MYXV specific reads from Δ*M062R* and wildtype MYXV infection showed that only the *M062R* gene was absent in samples infected with the Δ*M062R*

recombinant. Alignment files (i.e., BAM) from the first replicate from each of the 8 h Δ*M062R* and wildtype MYXV infection, was uploaded to igv.org/app/ for visualization. The dual genome reference was also uploaded and only the base pairs corresponding to the *M062R* gene were displayed.

References

1. Li XD, Wu J, Gao D, Wang H, Sun L, Chen ZJ. Pivotal roles of cGAS-cGAMP signaling in antiviral defense and immune adjuvant effects. Science. 2013;341(6152):1390-4.
2. Sun L, Wu J, Du F, Chen X, Chen ZJ. Cyclic GMP-AMP synthase is a cytosolic DNA sensor that activates the type I interferon pathway. Science. 2013;339(6121):786-91.
3. Wu J, Sun L, Chen X, Du F, Shi H, Chen C, et al. Cyclic GMP-AMP is an endogenous second messenger in innate immune signaling by cytosolic DNA. Science. 2013;339(6121):826-30.
4. Yoneyama M, Fujita T. RIG-I family RNA helicases: cytoplasmic sensor for antiviral innate immunity. Cytokine Growth Factor Rev. 2007;18(5-6):545-51.
5. Yoneyama M, Kikuchi M, Natsukawa T, Shinobu N, Imaizumi T, Miyagishi M, et al. The RNA helicase RIG-I has an essential function in double-stranded RNA-induced innate antiviral responses. Nat Immunol. 2004;5(7):730-7.
6. Nounamo B, Liem J, Cannon M, Liu J. Myxoma Virus Optimizes Cisplatin for the Treatment of Ovarian Cancer In Vitro and in a Syngeneic Murine Dissemination Model. Mol Ther Oncolytics. 2017;6:90-9.
7. Liu J, Wennier S, Zhang L, McFadden G. M062 is a host range factor essential for myxoma virus pathogenesis and functions as an antagonist of host SAMD9 in human cells. Journal of virology. 2011;85(7):3270-82.
8. Liu J, McFadden G. SAMD9 is an innate antiviral host factor with stress response properties that can be antagonized by poxviruses. Journal of virology. 2015;89(3):1925-31.
9. Georgana I, Sumner RP, Towers GJ, Maluquer de Motes C. Virulent Poxviruses Inhibit DNA Sensing by Preventing STING Activation. Journal of virology. 2018;92(10).
10. Dippel AB, Hammond MC. A Poxin on Both of Your Houses: Poxviruses Degrade the Immune Signal cGAMP. Biochemistry. 2019;58(19):2387-8.
11. Eaglesham JB, Pan Y, Kupper TS, Kranzusch PJ. Viral and metazoan poxins are cGAMP-specific nucleases that restrict cGAS-STING signalling. Nature. 2019;566(7743):259-63.
12. Eaglesham JB, McCarty KL, Kranzusch PJ. Structures of diverse poxin cGAMP nucleases reveal a widespread role for cGAS-STING evasion in host-pathogen conflict. Elife. 2020;9.
13. Hernaez B, Alonso G, Georgana I, El-Jesr M, Martin R, Shair KHY, et al. Viral cGAMP nuclease reveals the essential role of DNA sensing in protection against acute lethal virus infection. Sci Adv. 2020;6(38).
14. Meade N, Furey C, Li H, Verma R, Chai Q, Rollins MG, et al. Poxviruses Evade Cytosolic Sensing through Disruption of an mTORC1-mTORC2 Regulatory Circuit. Cell. 2018;174(5):1143-57 e17.
15. Meade N, King M, Munger J, Walsh D. mTOR Dysregulation by Vaccinia Virus F17 Controls Multiple Processes with Varying Roles in Infection. Journal of virology. 2019;93(15).

16. Cameron C, Hota-Mitchell S, Chen L, Barrett J, Cao JX, Macaulay C, et al. The complete DNA sequence of myxoma virus. Virology. 1999;264(2):298-318.
17. Liu J, Rothenburg S, McFadden G. The poxvirus C7L host range factor superfamily. Current opinion in virology. 2012;2(6):764-72.
18. Nounamo B, Li Y, O'Byrne P, Kearney AM, Khan A, Liu J. An interaction domain in human SAMD9 is essential for myxoma virus host-range determinant M062 antagonism of host anti-viral function. Virology. 2017;503:94-102.
19. Barrett JW, Shun Chang C, Wang G, Werden SJ, Shao Z, Barrett C, et al. Myxoma virus M063R is a host range gene essential for virus replication in rabbit cells. Virology. 2007;361(1):123-32.
20. Mekhedov SL, Makarova KS, Koonin EV. The complex domain architecture of SAMD9 family proteins, predicted STAND-like NTPases, suggests new links to inflammation and apoptosis. Biol Direct. 2017;12(1):13.
21. Unterholzner L, Keating SE, Baran M, Horan KA, Jensen SB, Sharma S, et al. IFI16 is an innate immune sensor for intracellular DNA. Nat Immunol. 2010;11(11):997-1004.
22. Li W, Avey D, Fu B, Wu JJ, Ma S, Liu X, et al. Kaposi's Sarcoma-Associated Herpesvirus Inhibitor of cGAS (KicGAS), Encoded by ORF52, Is an Abundant Tegument Protein and Is Required for Production of Infectious Progeny Viruses. Journal of virology. 2016;90(11):5329-42.
23. Hernaez B, Alonso-Lobo JM, Montanuy I, Fischer C, Sauer S, Sigal L, et al. A virus-encoded type I interferon decoy receptor enables evasion of host immunity through cell-surface binding. Nat Commun. 2018;9(1):5440.
24. Stuart JH, Sumner RP, Lu Y, Snowden JS, Smith GL. Vaccinia Virus Protein C6 Inhibits Type I IFN Signalling in the Nucleus and Binds to the Transactivation Domain of STAT2. PLoS pathogens. 2016;12(12):e1005955.
25. Postigo A, Ramsden AE, Howell M, Way M. Cytoplasmic ATR Activation Promotes Vaccinia Virus Genome Replication. Cell Rep. 2017;19(5):1022-32.
26. Rahman MM, Liu J, Chan WM, Rothenburg S, McFadden G. Myxoma virus protein M029 is a dual function immunomodulator that inhibits PKR and also conscripts RHA/DHX9 to promote expanded host tropism and viral replication. PLoS pathogens. 2013;9(7):e1003465.
27. Kerr PJ, Cattadori IM, Liu J, Sim DG, Dodds JW, Brooks JW, et al. Next step in the ongoing arms race between myxoma virus and wild rabbits in Australia is a novel disease phenotype. Proc Natl Acad Sci U S A. 2017;114(35):9397-402.
28. Wu J, Chen ZJ. Innate immune sensing and signaling of cytosolic nucleic acids. Annu Rev Immunol. 2014;32:461-88.
29. Unterholzner L, Sumner RP, Baran M, Ren H, Mansur DS, Bourke NM, et al. Vaccinia virus protein C6 is a virulence factor that binds TBK-1 adaptor proteins and inhibits activation of IRF3 and IRF7. PLoS pathogens. 2011;7(9):e1002247.
30. Benfield CT, Mansur DS, McCoy LE, Ferguson BJ, Bahar MW, Oldring AP, et al. Mapping the IkappaB kinase beta (IKKbeta)-binding interface of the B14 protein, a vaccinia virus inhibitor of IKKbeta-mediated activation of nuclear factor kappaB. J Biol Chem. 2011;286(23):20727-35.
31. Albarnaz JD, Ren H, Torres AA, Shmeleva EV, Melo CA, Bannister AJ, et al. Molecular mimicry of NF-kappaB by vaccinia virus protein enables selective inhibition of antiviral responses. Nat Microbiol. 2022;7(1):154-68.
32. Meng X, Chao J, Xiang Y. Identification from diverse mammalian poxviruses of host-range regulatory genes functioning equivalently to vaccinia virus C7L. Virology. 2008;372(2):372-83.
33. Perkus ME, Goebel SJ, Davis SW, Johnson GP, Limbach K, Norton EK, et al. Vaccinia virus host range genes. Virology. 1990;179(1):276-86.
34. Paludan SR, Bowie AG. Immune sensing of DNA. Immunity. 2013;38(5):870-80.

35. Xiao TS, Fitzgerald KA. The cGAS-STING pathway for DNA sensing. Mol Cell. 2013;51(2):135-9.
36. Shen YJ, Le Bert N, Chitre AA, Koo CX, Nga XH, Ho SS, et al. Genome-derived cytosolic DNA mediates type I interferon-dependent rejection of B cell lymphoma cells. Cell Rep. 2015;11(3):460-73.
37. Jakobsen MR, Olagnier D, Hiscott J. Innate immune sensing of HIV-1 infection. Curr Opin HIV AIDS. 2015;10(2):96-102.
38. de Weerd NA, Nguyen T. The interferons and their receptors--distribution and regulation. Immunol Cell Biol. 2012;90(5):483-91.
39. Yoshimura A, Naka T, Kubo M. SOCS proteins, cytokine signalling and immune regulation. Nat Rev Immunol. 2007;7(6):454-65.
40. Sarasin-Filipowicz M, Wang X, Yan M, Duong FH, Poli V, Hilton DJ, et al. Alpha interferon induces long-lasting refractoriness of JAK-STAT signaling in the mouse liver through induction of USP18/UBP43. Mol Cell Biol. 2009;29(17):4841-51.
41. Ivashkiv LB, Donlin LT. Regulation of type I interferon responses. Nat Rev Immunol. 2014;14(1):36-49.
42. Seo GJ, Yang A, Tan B, Kim S, Liang Q, Choi Y, et al. Akt Kinase-Mediated Checkpoint of cGAS DNA Sensing Pathway. Cell Rep. 2015;13(2):440-9.
43. Li S, Qian N, Jiang C, Zu W, Liang A, Li M, et al. Gain-of-function genetic screening identifies the antiviral function of TMEM120A via STING activation. Nat Commun. 2022;13(1):105.
44. Huang L, Xu W, Liu H, Xue M, Liu X, Zhang K, et al. African Swine Fever Virus pI215L Negatively Regulates cGAS-STING Signaling Pathway through Recruiting RNF138 to Inhibit K63-Linked Ubiquitination of TBK1. J Immunol. 2021;207(11):2754-69.
45. Thomas ME, 3rd, Abdelhamed S, Hiltenbrand R, Schwartz JR, Sakurada SM, Walsh M, et al. Pediatric MDS and bone marrow failure-associated germline mutations in SAMD9 and SAMD9L impair multiple pathways in primary hematopoietic cells. Leukemia. 2021.
46. Meng X, Zhang F, Yan B, Si C, Honda H, Nagamachi A, et al. A paralogous pair of mammalian host restriction factors form a critical host barrier against poxvirus infection. PLoS pathogens. 2018;14(2):e1006884.
47. Zhang LK, Chai F, Li HY, Xiao G, Guo L. Identification of host proteins involved in Japanese encephalitis virus infection by quantitative proteomics analysis. J Proteome Res. 2013;12(6):2666-78.
48. Kane M, Zang TM, Rihn SJ, Zhang F, Kueck T, Alim M, et al. Identification of Interferon-Stimulated Genes with Antiretroviral Activity. Cell Host Microbe. 2016;20(3):392-405.
49. Wang J, Dupuis C, Tyring SK, Underbrink MP. Sterile alpha Motif Domain Containing 9 Is a Novel Cellular Interacting Partner to Low-Risk Type Human Papillomavirus E6 Proteins. PLoS One. 2016;11(2):e0149859.
50. Wu JJ, Li W, Shao Y, Avey D, Fu B, Gillen J, et al. Inhibition of cGAS DNA Sensing by a Herpesvirus Virion Protein. Cell Host Microbe. 2015;18(3):333-44.
51. Smallwood SE, Rahman MM, Smith DW, McFadden G. Myxoma virus: propagation, purification, quantification, and storage. Curr Protoc Microbiol. 2010;Chapter 14:Unit 14A 1.
52. Illumina. bcl2fastq2 and bcl2fastq Conversion Software Downloads [Available from: https://support.illumina.com/sequencing/sequencing_software/bcl2fastq-conversion-software/downloads.html.
53. Babraham Institute BB. FastQC: A Quality Control tool for High Throughput Sequence Data [Available from: http://www.bioinformatics.babraham.ac.uk/projects/fastqc/.
54. Dobin A, Davis CA, Schlesinger F, Drenkow J, Zaleski C, Jha S, et al. STAR: ultrafast universal RNA-seq aligner. Bioinformatics. 2013;29(1):15-21.

713 55. Garcia-Alcalde F, Okonechnikov K, Carbonell J, Cruz LM, Gotz S, Tarazona S, et al.
714 Qualimap: evaluating next-generation sequencing alignment data. Bioinformatics.
715 2012;28(20):2678-9.
716 56. Pertea M, Pertea GM, Antonescu CM, Chang TC, Mendell JT, Salzberg SL. StringTie
717 enables improved reconstruction of a transcriptome from RNA-seq reads. Nat Biotechnol.
718 2015;33(3):290-5.
719 57. Love MI, Huber W, Anders S. Moderated estimation of fold change and dispersion for
720 RNA-seq data with DESeq2. Genome Biol. 2014;15(12):550.
721

Figure 1.

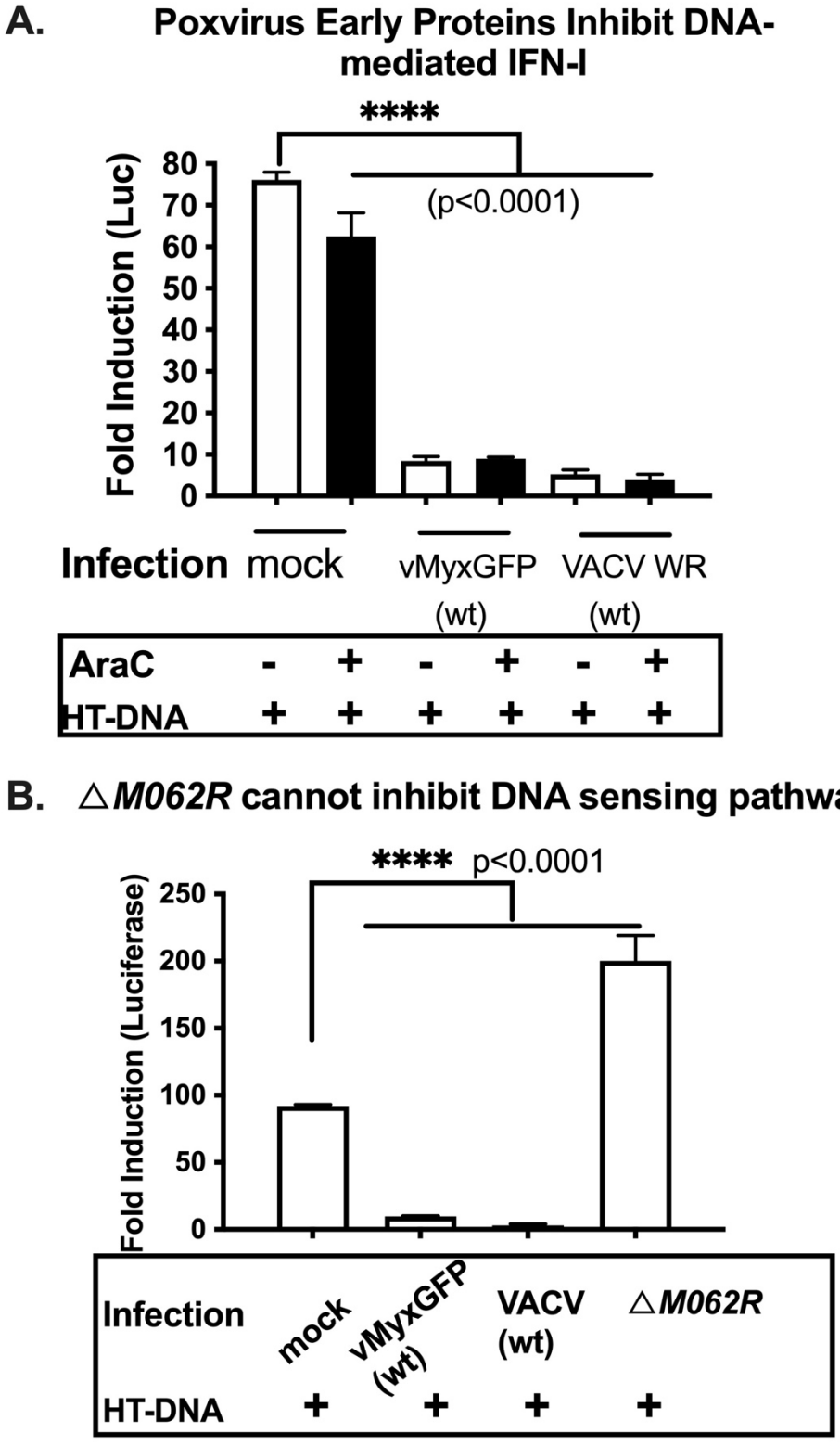

Figure 2.

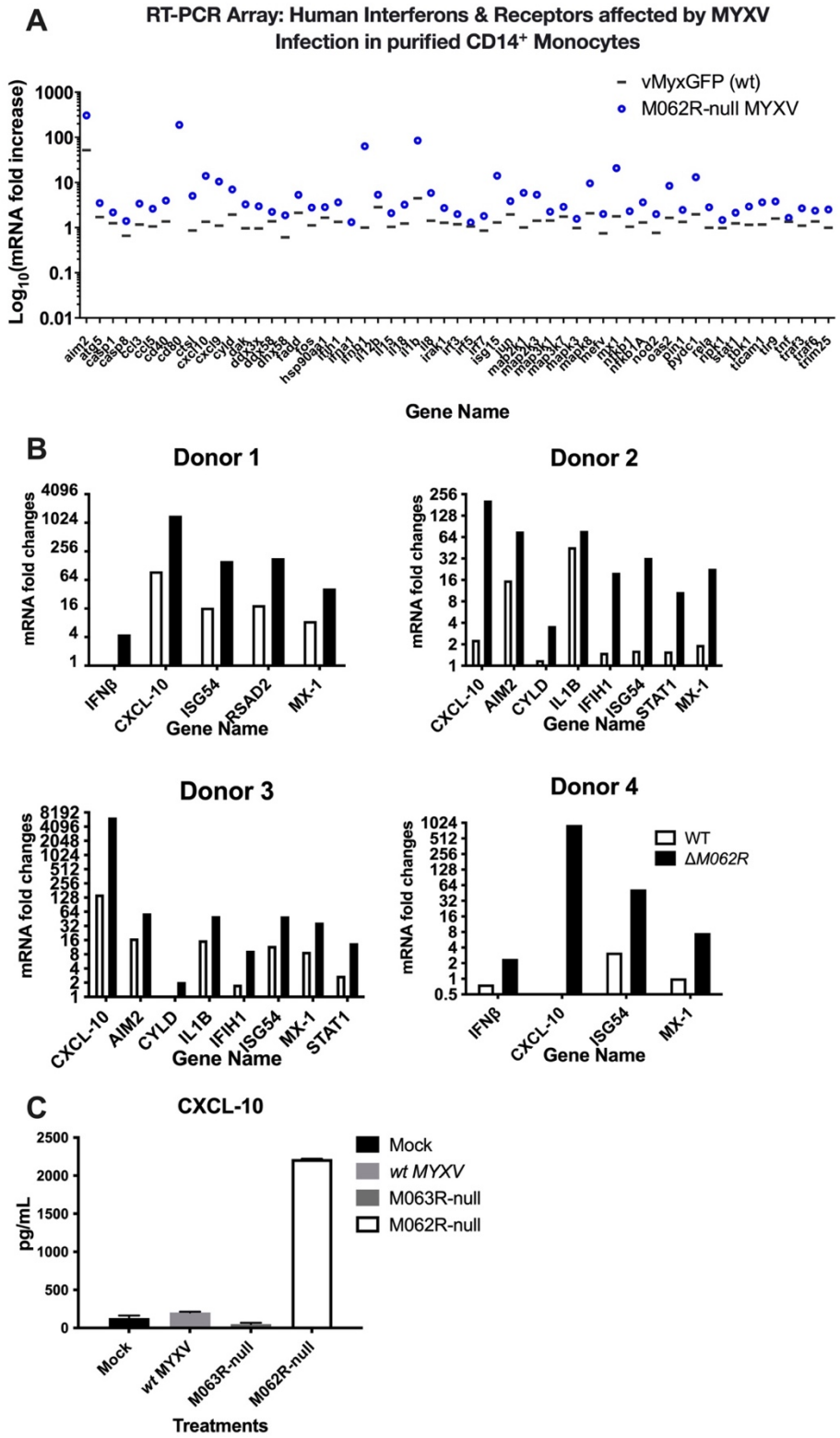

Figure 3.

A.

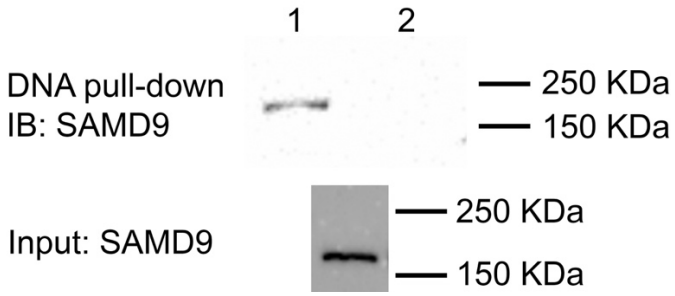

B.

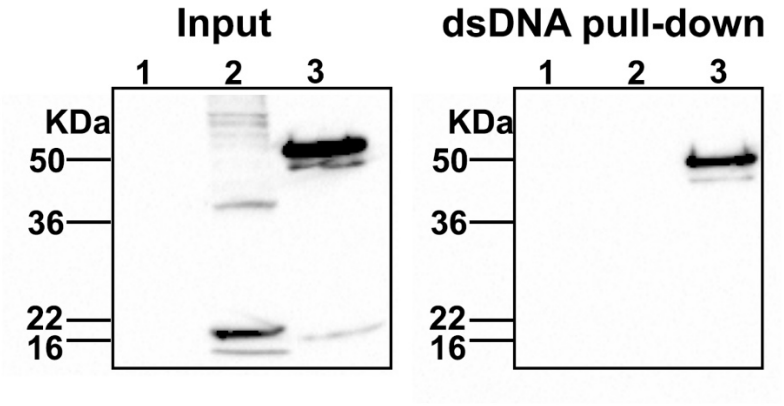

C.

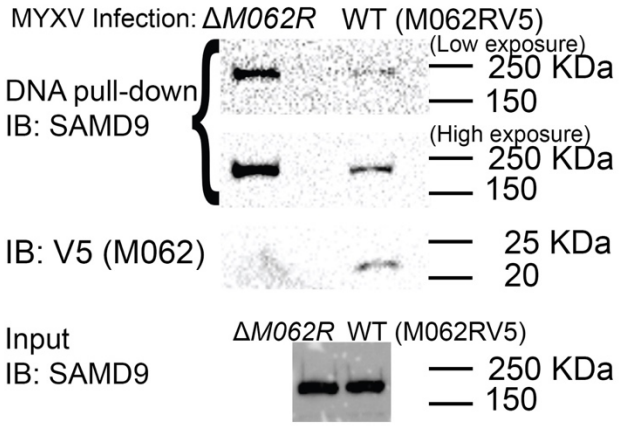

Figure 4.

A.

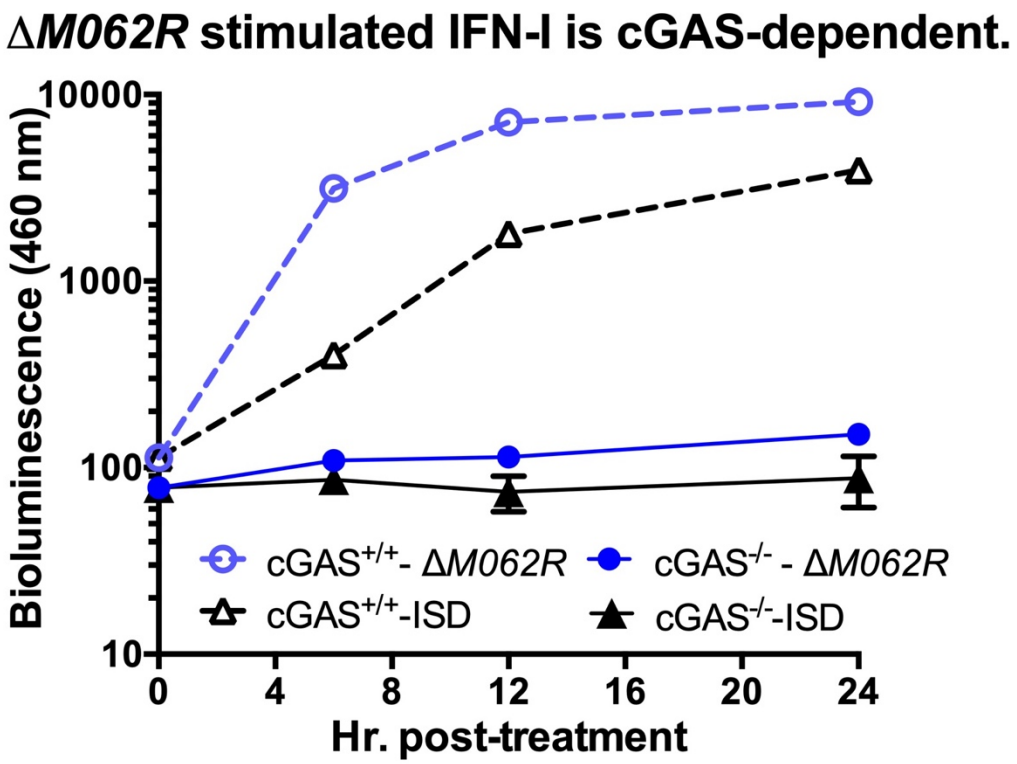

B.

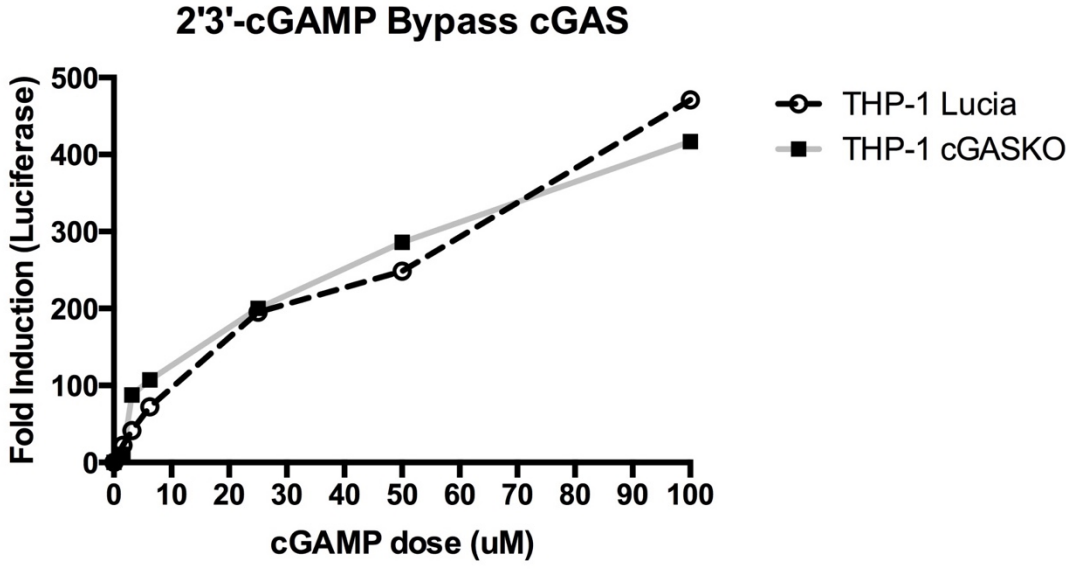

17

Figure 5.

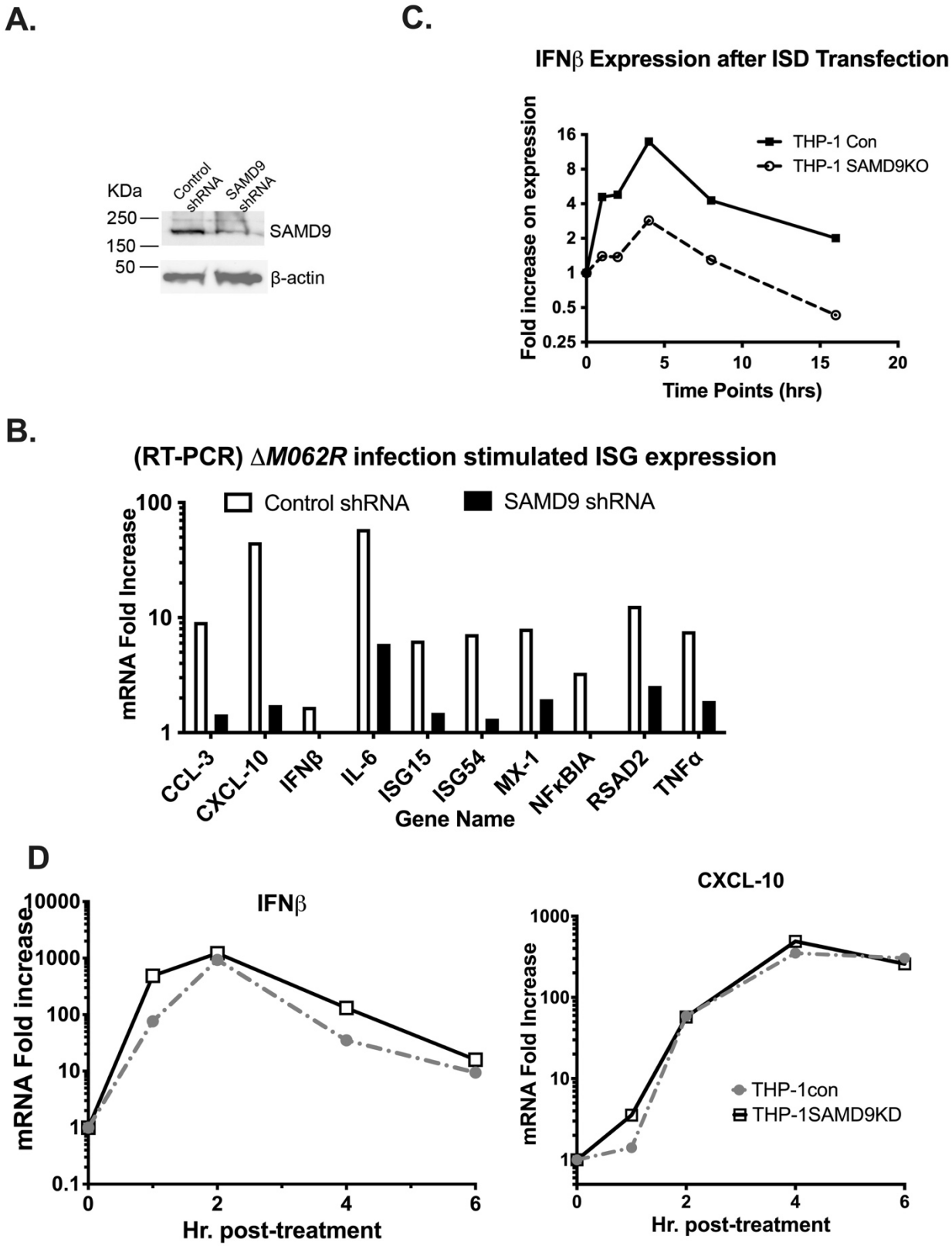

18

Figure 6.

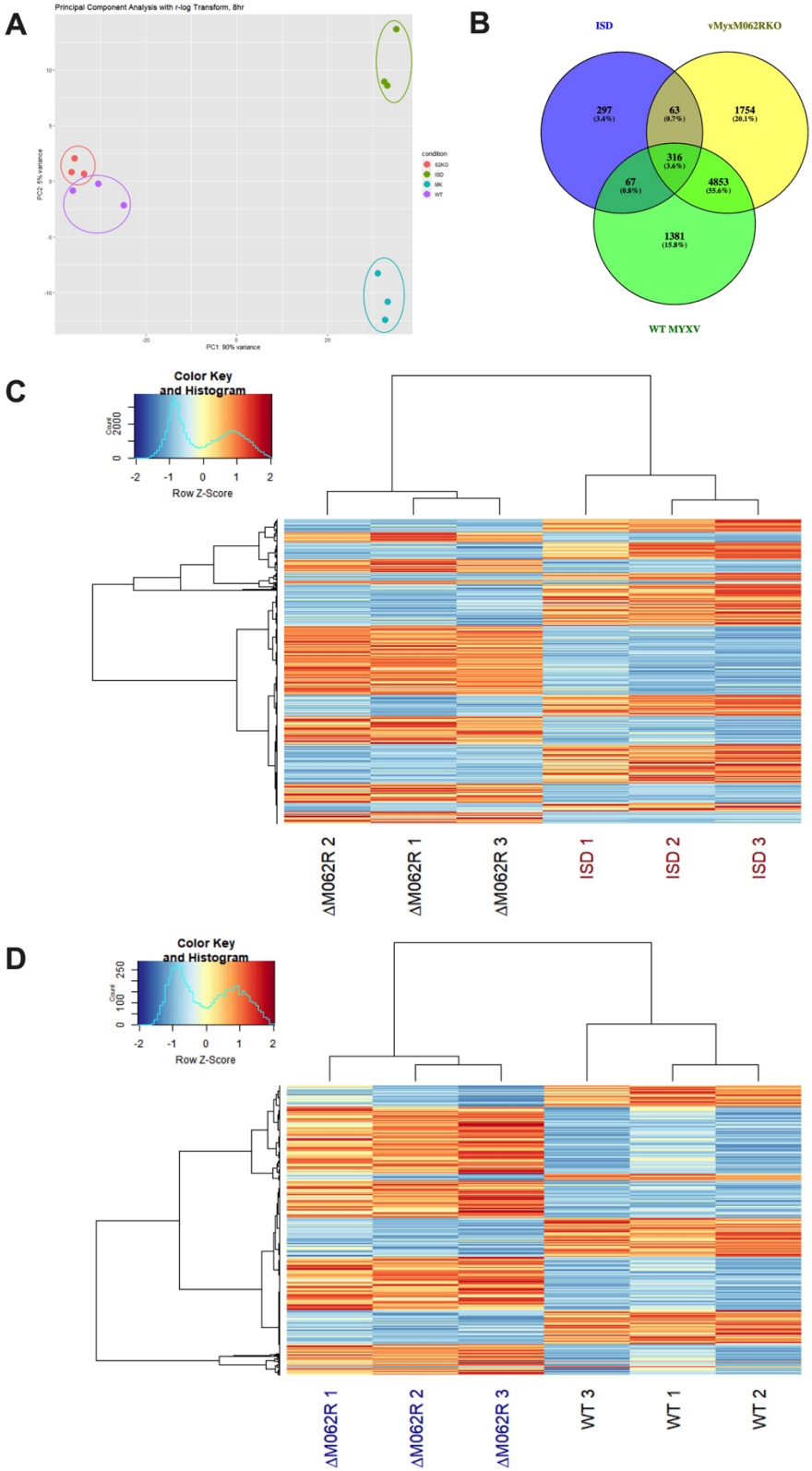

Figure 6. Continued

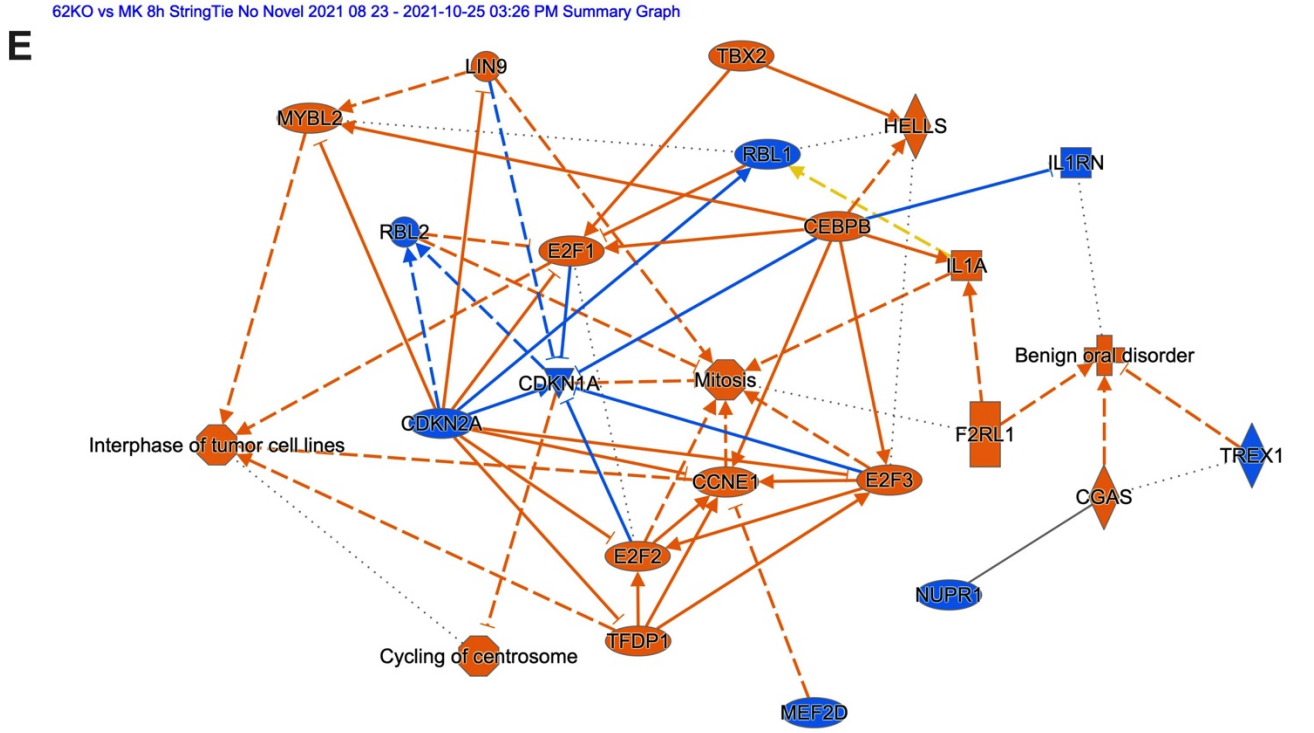

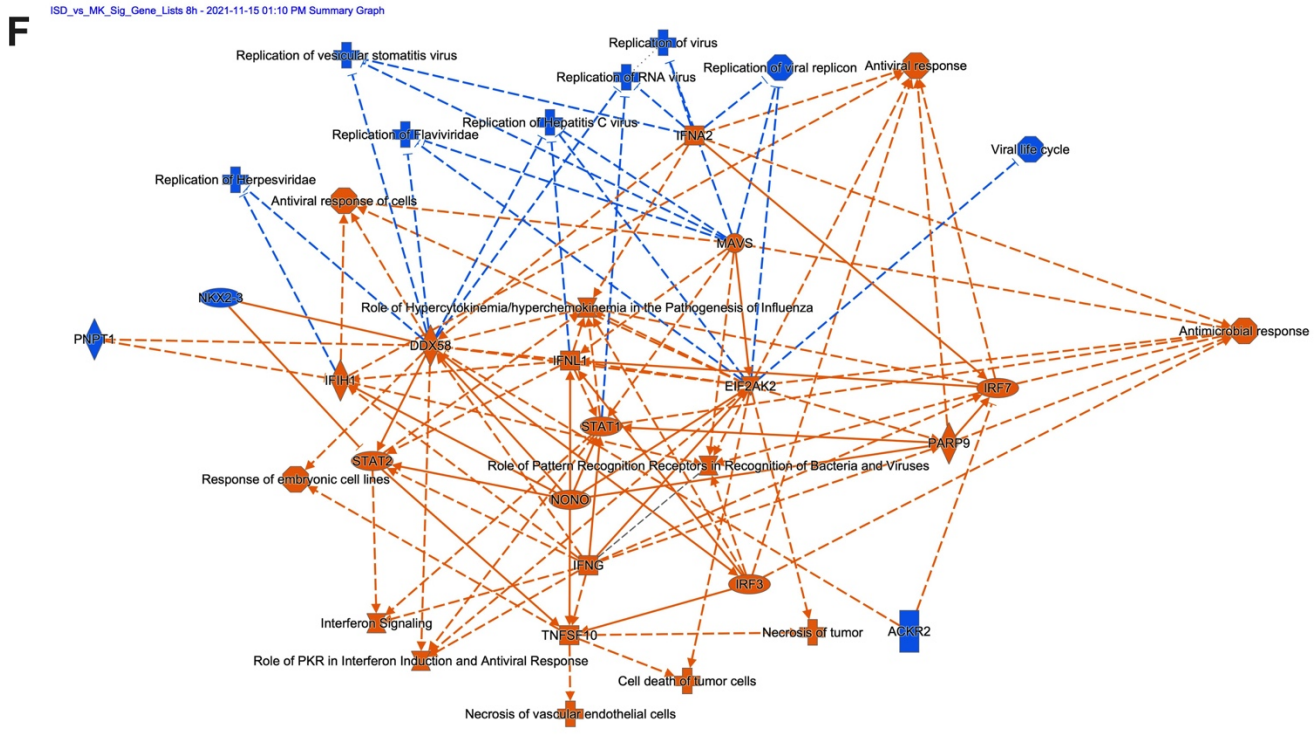

Figure 7.

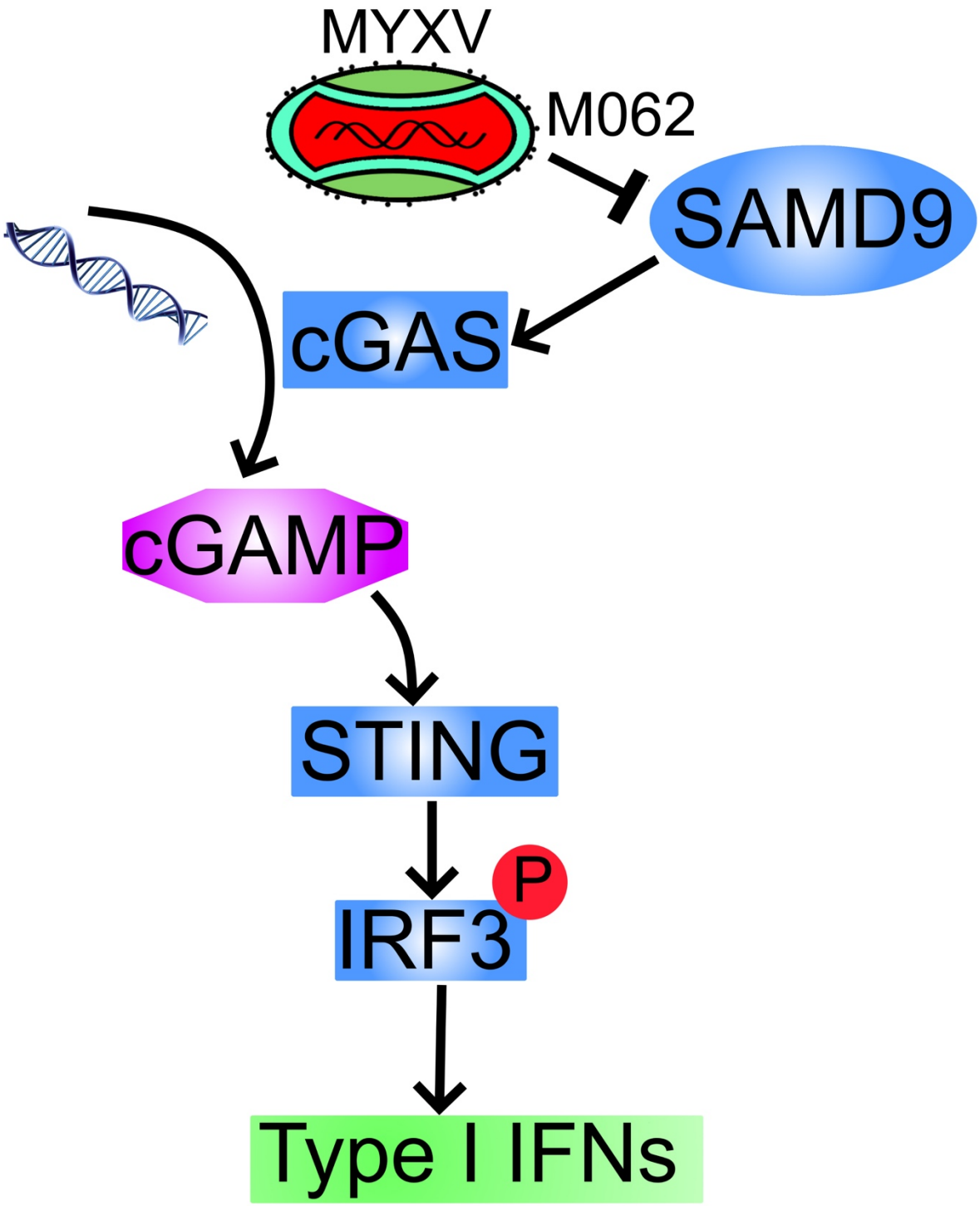

Supplemental Figure 1.

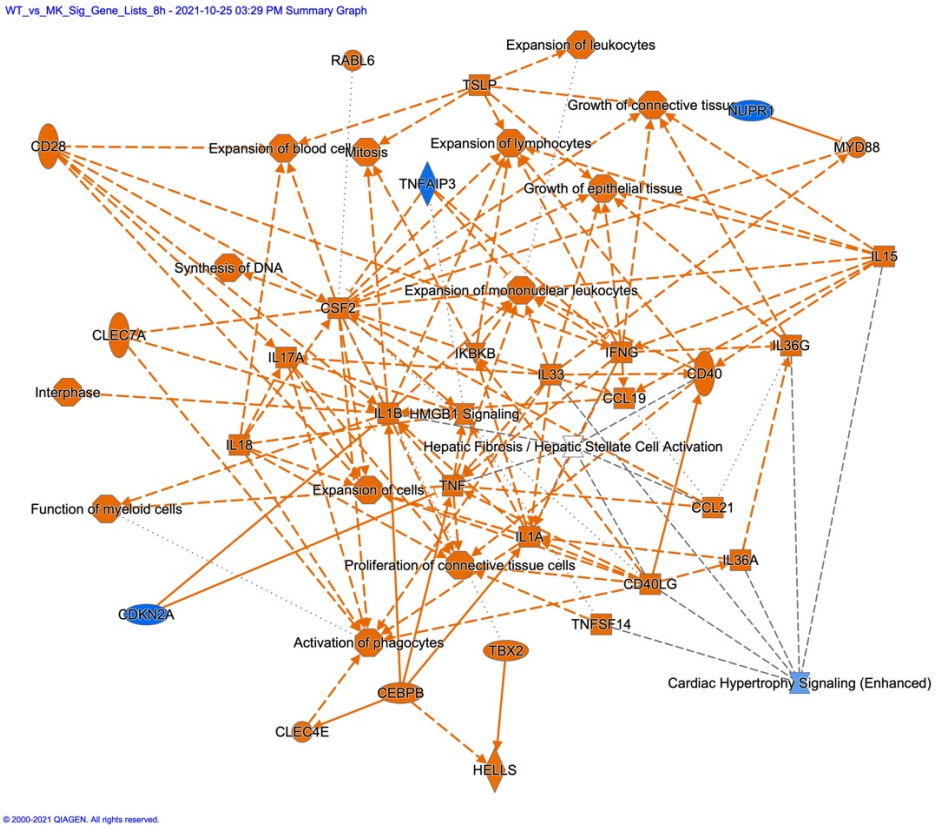

Supplemental Figure 2.

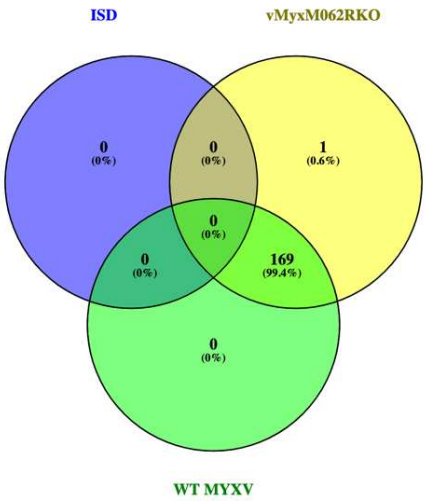

Supplemental Figure 3.

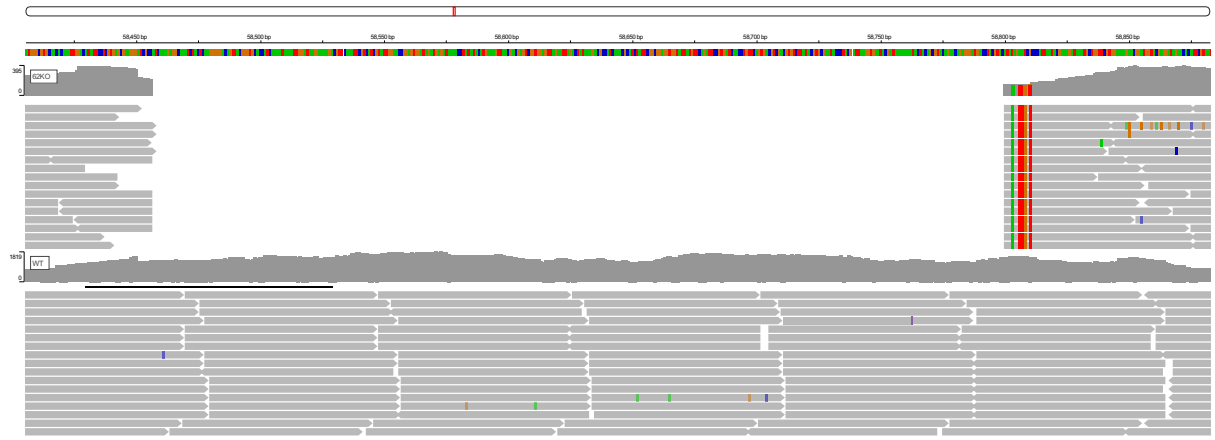

Table 1. Real-time PCR Primer sequences

Target Gene	Primer sequences
AIM2	Forward (Fwd): 5'- CTCCTGAGTCCTCTGCTAGTTA -3'
	Reverse (Rev): 5'- ACTCTCCATCTGACAACTTTGG -3'
CXCL-10	Fwd 5'- CTG TAC CTG CAT CAG CAT TAG TA -3'
	Rev 5'- GAC ATC TCT TCT CAC CCT TCT TT -3'
CYLD	Fwd 5'- gtgggctgtcctgtgaaagta -3'
	Rev 5'- aagctgtttcccttggtaca -3'
IFIH1	Fwd 5'- accaaatacaggagccatgc -3'
	Rev 5'- gcgatttccttcttttgcag-3'
IFN B1	Fwd 5'- GCC ATC AGT CAC TTA AAC AGC -3'
	Rev 5'- GAA ACT GAA GAT CTC CTA GCC T -3'
IL1B	Fwd 5'- AAGTACCTGAGCTCGCCAGTGAAA -3'
	Rev 5'- TTGCTGTAGTGGTGGTCGGAGATT -3'
ISG15	Fwd 5'- gcgaactcatctttgccagt -3'
	Rev 5'- cttcagctctgacaccgaca -3'
ISG54	Fwd 5'- AGCGAAGGTGTGCTTTGAGA -3'
	Rev 5'- GAGGGTCAATGGCGTTCTGA -3'
MX-1	Fwd 5'- ctcccactccctgaaatctg -3'
	Rev 5'- ttcggaaacaaccatcttcc -3'
NFκB1A	Fwd 5'- CCCTACACCTTGCCTGTGAG -3'
	Rev 5'- TGACATCAGCACCCAAGGAC -3'
RSAD2	Fwd 5'- AGT GCA ACT ACA AAT GCG GC -3'
	Rev 5'- CTT GCC CAG GTA TTC TCC CC -3'
STAT1	Fwd 5'- CTA GTG GAG TGG AAG CGG AG -3'
	Rev 5'- CAC CAC AAA CGA GCT CTG AA -3'
TNFα	Fwd 5'- TCCCCAGGGACCTCTCTCTA -3'
	Rev 5'- GAGGGTTTGCTACAACATGGG -3'

62 **Table 2. Differentially expressed viral genes in Δ*M062R* and wildtype MYXV in**
63 **human macrophages**

Uniprot ID	Gene ID	Expression kinetics	logFC	p-Value	Conservation within poxviruses
MYXV_gp005	M003.2L	Unknown	0.8	1.34e-03	Sermi-conserved
MYXV_gp007	M004.1L	Late	0.801	3.22e-03	Unique
MYXV_gp008	M005L (M-T5)	Early	0.835	9.9e-05	Sermi-conserved
MYXV_gp009	M006L	Early	0.928	6.18e-6	Sermi-conserved
MYXV_gp011	M008L	Early	0.6980	7.88e-05	Sermi-conserved
MYXV_gp012	M008.1L	Late	0.901	8.94e-06	Uniuqe
MYXV_gp015	M011L	Early	0.637	8.45e-04	Sermi-conserved
MYXV_gp017	M013L	Early	0.489	4.18e-03	Unique
MYXV_gp022	M018L	Early	0.544	4.39e-03	Sermi-conserved
MYXV_gp023	M019L	Late	0.59	3.57e-03	Conserved VACV F9L
MYXV_gp028	M024L	Early	0.883	4.32e-06	Sermi-conserved
MYXV_gp031	M027L	Late	0.93	1.97e-06	Conserved VACV E1L
MYXV_gp032	M028L	Late	0.617	4.87e-04	Conserved VACV E2L
MYXV_gp035	M031R	Early	0.429	1.77e-03	Sermi-conserved
MYXV_gp036	M032R	Late	0.604	1.78e-04	Conserved
MYXV_gp038	M034L	Early	0.67	3.94e-04	Conserved
MYXV_gp053	M049R	Early	0.39	5.72e-03	Sermi-conserved
MYXV_gp055	M051R	Unknown	0.54	1.18e-03	Sermi-conserved VACVG6R
MYXV_gp057	M053R	Intermediate	0.746	1.27e-04	Conserved VACV G8R
MYXV_gp058	M054R	Late	0.824	2.44e-05	Sermi-conserved VACV G9R
MYXV_gp059	M055R	Late	0.643	5.12e-04	Conserved VACV L1R
MYXV_gp062	M058R	Late	0.507	1.77e-03	Conserved VACV L4R
MYXV_gp066	M062R	Early/Late	-3.95	2.72e-88	Conserved VACV C7L
MYXV_gp067	M063R	Early/Late	0.56	5.56e-04	Sermi-conserved VACV C7L
MYXV_gp072	M068R	Early or Intermediate	0.416	5.82e-03	Conserved VACV J6R
MYXV_gp077	M073R	Early	0.6450	2.36e-04	Sermi-conserved VACV H5R
MYXV_gp078	M074R	Early/Late	0.8280	1.5e-05	Conserved VACV H6R
MYXV_gp079	M075R	Early	0.505	2.3e-03	Sermi-conserved VACV H7R
MYXV_gp088	M084R	Early	0.774	3.37e-05	Conserved VACV D9R
MYXV_gp106	M102L	Late	-0.8610	4.51e-04	Sermi-conserved VACV A13L
MYXV_gp107	M103L	Late	-1.16	3.54e-05	Conserved VACV A14L
MYXV_gp110	M106L	Late	-0.6520	4.81e-04	Conserved VACV A16L
MYXV_gp111	M107L	Late	-0.8240	1.57e-03	Sermi-conserved VACV A17L
MYXV_gp112	M108R	Intermediate	0.969	6.44e-06	Conserved VACV A18R
MYXV_gp114	M110L	Late	0.802	9.72e-04	Conserved VACV A21L
MYXV_gp119	M115L	Late	0.918	1.23e-06	Sermi-conserved VACV A27L
MYXV_gp120	M116L	Late	1.02	2.7e-07	Conserved VACV A28L
MYXV_gp121	M117L	Early	0.535	1.11e-03	Conserved VACV A29L
MYXV_gp122	M118L	Late	0.678	2.5e-04	Conserved VACV A30L
MYXV_gp123	M119L	Early	0.582	1.38e-03	Unique
MYXV_gp126	M122R	Late	0.888	1.02e-04	Sermi-conserved VACV A34R
MYXV_gp133	M129R	Early	0.615	1.37e-03	Sermi-conserved VACV E7R
MYXV_gp134	M130R	Early	0.515	9.06e-04	Unique
MYXV_gp140	M136R	Late?	1.4	5.54e-11	Unique VACV A52R
MYXV_gp144	M140R	Early	0.599	1.06e-03	Sermi-conserved VACV A55R
MYXV_gp145	M141R	Early	0.734	2.93e-04	Unique
MYXV_gp148	M144R	Early	0.463	4.99e-03	Sermi-conserved VACV N1L
MYXV_gp153	M150R	Early	0.565	1.03e-03	Unique VACV C9L
MYXV_gp154	M151R	Early	0.792	9.40e-05	Sermi-conserved VACV SPI-2
MYXV_gp155	M152R	Early	0.843	5.60e-05	Unique
MYXV_gp158	M156R	Early	0.638	2.51e-04	Sermi-conserved VACV K3L
MYXV_gp159	M008.1L	Late	0.893	9.81e-06	Unique
MYXV_gp160	M008L	Early	0.694	8.45e-05	Sermi-conserved
MYXV_gp162	M006R	Early	0.931	5.51e-06	Sermi-conserved
MYXV_gp163	M005R (M-T5)	Early/Late	0.833	1.05e-04	Sermi-conserved
MYXV_gp164	M004.1L	Late	0.791	3.37e-03	Unique
MYXV_gp166	M003.2L	Unknown	0.787	1.45e-03	Sermi-conserved